Accepted Manuscript

Antifungal Benzo[b]thiophene 1,1-dioxide IMPDH Inhibitors Exhibit Pan-Assay Interference (PAINS) Profiles

Lalith K. Kummari, Mark S. Butler, Emily Furlong, Ross Blundell, Amanda Nouwens, Alberto B. Silva, Ulrike Kappler, James A. Fraser, Bostjan Kobe, Matthew A. Cooper, Avril A.B. Robertson
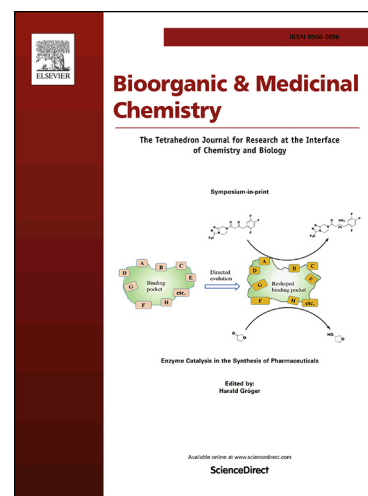
Please cite this article as: Kummari, L.K., Butler, M.S., Furlong, E., Blundell, R., Nouwens, A., Silva, A.B., Kappler, U., Fraser, J.A., Kobe, B., Cooper, M.A., Robertson, A.A.B., Antifungal Benzo[b]thiophene 1,1-dioxide IMPDH Inhibitors Exhibit Pan-Assay Interference (PAINS) Profiles, *Bioorganic & Medicinal Chemistry* (2018), doi: https://doi.org/10.1016/j.bmc.2018.09.004

Antifungal Benzo[b]thiophene 1,1-dioxide IMPDH Inhibitors Exhibit Pan-Assay Interference (PAINS) Profiles

Lalith K. Kummari,[1-3] Mark S. Butler,[3] Emily Furlong,[3] Ross Blundell,[2] Amanda Nouwens,[1] Alberto B. Silva,[3, 5] Ulrike Kappler,[4] James A. Fraser,[2] Bostjan Kobe,[2, 3] Matthew A. Cooper,[3] Avril A. B. Robertson[1, 3*]

[1]School of Chemistry and Molecular Biosciences, The University of Queensland, Brisbane, Queensland 4072, Australia

[2]Australian Infectious Diseases Research Centre, School of Chemistry and Molecular Biosciences, The University of Queensland, Brisbane, QLD 4072, Australia

[3]Institute for Molecular Bioscience, The University of Queensland, Brisbane, Queensland 4072, Australia

[4]Centre for Metals in Biology, School of Chemistry and Molecular Biosciences, The University of Queensland, Brisbane, Queensland 4072, Australia

[5]AC Immune SA, EPFL Innovation Park, CH-1015 Lausanne, Switzerland.

*Corresponding author:

Professor Avril A. B. Robertson PhD GCHEd

Biotechnology Program Director,

School of Chemistry and Molecular Biosciences,

Affiliate of the Institute for Molecular Bioscience,

The University of Queensland, St Lucia, QLD, 4072, AUSTRALIA

Phone: +61 7 3346 2204, Email: a.robertson3@uq.edu.au

ABSTRACT

Fungi cause serious life-threatening infections in immunocompromised individuals and current treatments are now complicated by toxicity issues and the emergence of drug resistant strains. Consequently, there is a need for development of new antifungal drugs. Inosine monophosphate dehydrogenase (IMPDH), a key component of the *de novo* purine biosynthetic pathway, is essential for growth and virulence of fungi and is a potential drug target. In this study, a high-throughput screen of 114,000 drug-like compounds against *Cryptococcus neoformans* IMPDH was performed. We identified three 3-((5-substituted)-1,3,4-oxadiazol-2-yl)thio benzo[*b*]thiophene 1,1-dioxides that inhibited *Cryptococcus* IMPDH and also possessed whole cell antifungal activity. Analogs were synthesized to explore the SAR of these hits. Modification of the fifth substituent on the 1,3,4-oxadiazole ring yielded compounds with nanomolar *in vitro* activity, but with associated cytotoxicity. In contrast, two analogs generated by substituting the 1,3,4-oxadiazole ring with imidazole and 1,2,4-triazole gave reduced IMPDH inhibition *in vitro,* but were not cytotoxic. During enzyme kinetic studies in the presence of DTT, nucleophilic attack of a free thiol occurred with the benzo[*b*]thiophene 1,1-dioxide. Two representative compounds with substitution at the 5 position of the 1,3,4-oxadiazole ring, showed mixed inhibition in the absence of DTT. Incubation of these compounds with *Cryptococcus* IMPDH followed by mass spectrometry analysis showed non-specific and covalent binding with IMPDH at multiple cysteine residues. These results support recent reports that the benzo[*b*]thiophene 1,1-dioxides moiety as PAINS (pan-assay interference compounds) contributor.

Keywords: High-throughput screening; IMPDH inhibitor; antifungal; PAINS; mass spectrometry; *Cryptococcus neoformans*.

2

1. Introduction

The Fungal Infection Trust has estimated that approximately 300 million people worldwide are afflicted with serious fungal infections.[1] Many of these pathogenic fungi are opportunistic and infect when the human immune system is compromised due to HIV/AIDS, anticancer chemotherapy or immunosuppressant treatment during organ transplantation. *Aspergillus fumigatus*, *Candida albicans* and *Cryptococcus neoformans* are among the most common fungal pathogens and are associated with highest mortality rates in immunocompromised populations.[2,3]

According to the Center for Disease Control and Prevention, nearly 220,000 new cases of cryptococcal meningitis occur each year with a fatality rate of >50%.[4] *Cryptococcus* infection occurs via inhaled spores that cause pulmonary infection in the lung alveoli. Later, the infection spreads to other parts of the body. Fungal cells that cross the blood brain barrier infect the meningeal membrane that protects the spinal cord and the brain. Resulting inflammation of the meninges causes cryptococcal meningitis, which is fatal unless treated.[5,6] The recommended treatment for cryptococcal meningitis is a combination antifungal therapy that uses amphotericin B deoxycholate and flucytosine, which is followed by life-long maintenance therapy with fluconazole to prevent reinfection. Amphotericin B therapy is associated with nephrotoxicity and infusion-related reactions such as chest pain, dyspnea, hypoxia, flushing, and urticaria.[7] Flucytosine and fluconazole cause adverse gastrointestinal effects and are toxic to bone marrow.[8,9] Moreover, the increasing resistance acquired by *C. neoformans* is making available treatments less effective. Given the limitations of existing antifungal therapeutics, there is a need to consider new approaches and targets.[10]

One such potential target is inosine monophosphate dehydrogenase (IMPDH), an enzyme of the purine metabolic pathway. IMPDH forms a homotetramer that catalyses the two-step

3

conversion of inosine-5′-monophosphate (IMP) to xanthosine-5′-monophosphate (XMP) using nicotinamide adenine dinucleotide (NAD) as a cofactor (**Figure 1**).[11] Deletion of the *IMD1* gene encoding IMPDH in *C. neoformans* leads to guanine auxotrophy and virulence factor production defects. Moreover, the mutant was avirulent in two animal infection models.[12] While *C. neoformans* is susceptible to the human IMPDH inhibitor mycophenolic acid (MPA), this well-known drug also targets the human IMPDH isoforms as an immunosuppressant. In treating immunocompromised individuals, the immunosuppressant properties of known IMPDH inhibitors, such as MPA, would clearly be detrimental to health and therefore discovery of fungal specific IMPDH inhibitors is essential. Both the crystal structure of *Cryptococcus* IMPDH, and kinetic data have revealed significant differences between this fungal enzyme and its human counterparts, providing an opportunity to produce novel, species-specific inhibitors.[12]

Step 1:

Step 2:
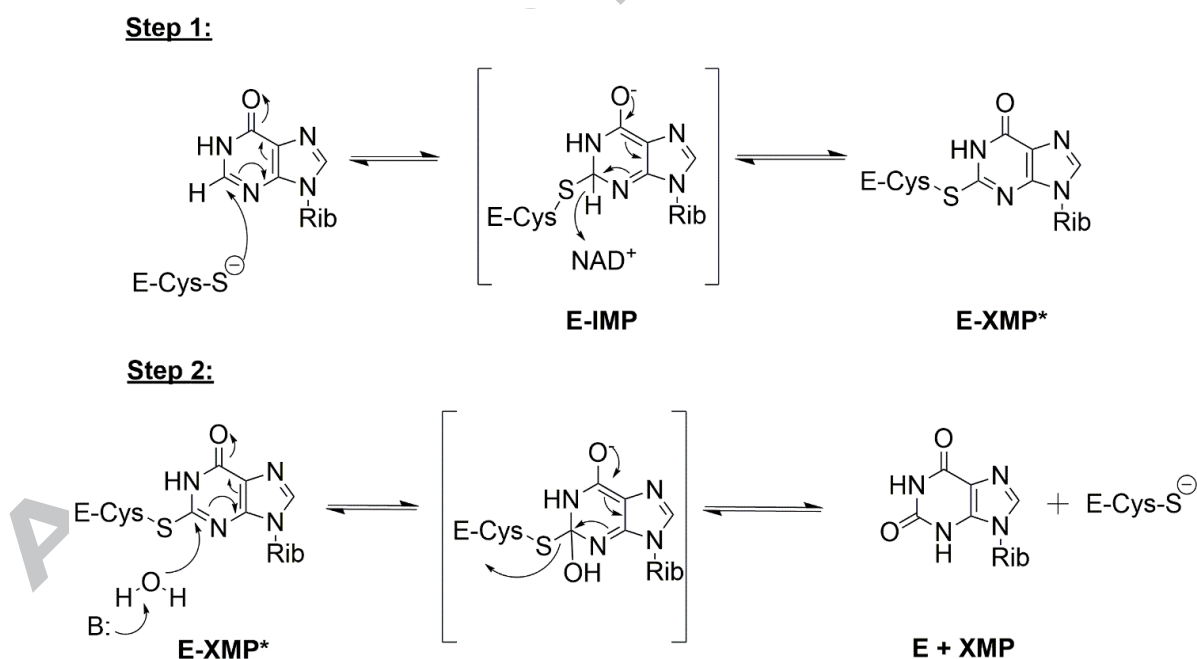
Figure 1. Two step mechanism for the conversion of IMP to XMP catalysed by IMPDH.

In this study, we highlight a set of inhibitors of *Cryptococcus* IMPDH identified using an enzyme inhibition assay adapted for high-throughput screening conducted with 114,000 drug-

4

like compounds from the Walter and Eliza Hall Compound Collection. Out of the screening, a hit-set of three molecules was identified comprising 1,3,4-oxadiazole ring attached to a benzothiophene-1,1-dioxide moiety *via* thioether group linkage. In addition to their unique structure and under-explored biological activity, they had potent inhibitory activity against *Cryptococcus* IMPDH and significant antifungal activity. Fifteen analogs were synthesized by modification of the aromatic group at the fifth position of the 1,3,4-oxadiazole ring moiety, to find selective *Cryptococcus* IMPDH inhibitors with potent antifungal activity. The observed IC$_{50}$ values against *Cryptococcus* IMPDH were consistent across all synthesized compounds and displayed potent antifungal activity. Modification of the 1,3,4-oxadiazole ring to imidazole or 1,3,4-triazole led to the loss of *Cryptococcus* IMPDH inhibition and antifungal activity. Mass spectrometry studies of *Cryptococcus* IMPDH incubated with one of the compounds showed nucleophilic attack of the cysteine thiolate anion at the C3-position of benzo[*b*]thiophene 1,1-dioxide. This reactivity also caused compound breakdown when performing kinetics studies in the presence of dithiothreitol (DTT). Consistent with our findings, Dahlin et al., recently reported that benzo[*b*]thiophene 1,1-dioxides were assay interfering compounds (PAINS).[13-16]
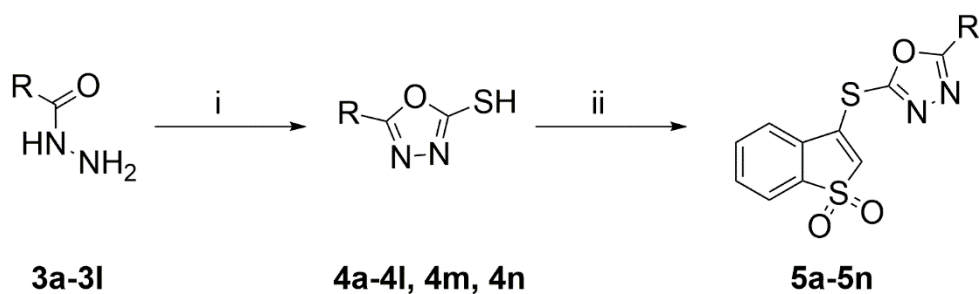
2. Results and discussion

2.1. Chemistry

To identify inhibitors of *Cryptococcus* IMPDH, the Walter and Eliza Hall Compound Collection (114,000 drug-like compounds) was screened using a spectrophotometric assay to measure the amount of NADH produced by IMPDH enzymatic activity. A 3-((5-substituted)-1,3,4-oxadiazol-2-yl)thio benzo[*b*]thiophene 1,1-dioxide series of hits was identified, with IC$_{50}$ values between 1 and 2 μM. On the basis of *in silico* docking studies to improve enzyme inhibition and antifungal activity, substitution at position 5 of the 1,3,4-oxadiazole ring was investigated. The synthetic route involved coupling 5-substitued 1,3,4-oxadiazole-2-thiol

5

intermediates with 3-bromo benzo[*b*]thiophene 1,1-dioxide (**2**) with copper iodide catalyst and benzotriazole under basic conditions (potassium *tert*-butoxide or Cs_2CO_3) in DMSO. These conditions had not previously been investigated with heteroaromatic thiols but afforded the desired compounds **5a-5o** in good yields (**Scheme 2**).[17] The *N*-acetyl modified compound **5o** was synthesized from compound **5n** by acetylation of amino groups using acetyl chloride and Et_3N as the base, in THF as the solvent.
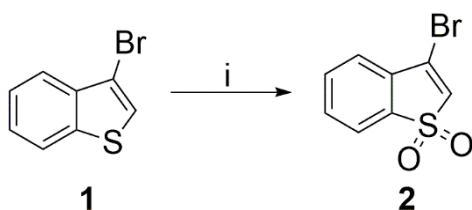
Scheme 1. Synthetic route of intermediate 2. Reagents and conditions: (i) *m*-CPBA, DCM, rt

3-Bromo benzo[*b*]thiophene 1,1-dioxide (**2**) was synthesized by oxidization of commercially available 3-bromo benzo[b]thiophene (**1**) using *m*-CPBA (**Scheme 1**). Required 5-substitued 1,3,4-oxadiazole-2-thiol intermediates were purchased commercially or synthesized by cyclization of the respective acid hydrazide using carbon disulfide in DMF, as reported by Mohammad Soleiman-Beigi et al. (**Scheme 2**).[18] However, an alternative method was needed to cyclize the cyclohexane carbohydrazide (**3e**) using carbon disulfide in ethanol, followed by addition of potassium hydroxide to give 5-(cyclohexyl)-1,3,4-oxadiazole-2-thiol (**4e**).[19,20]
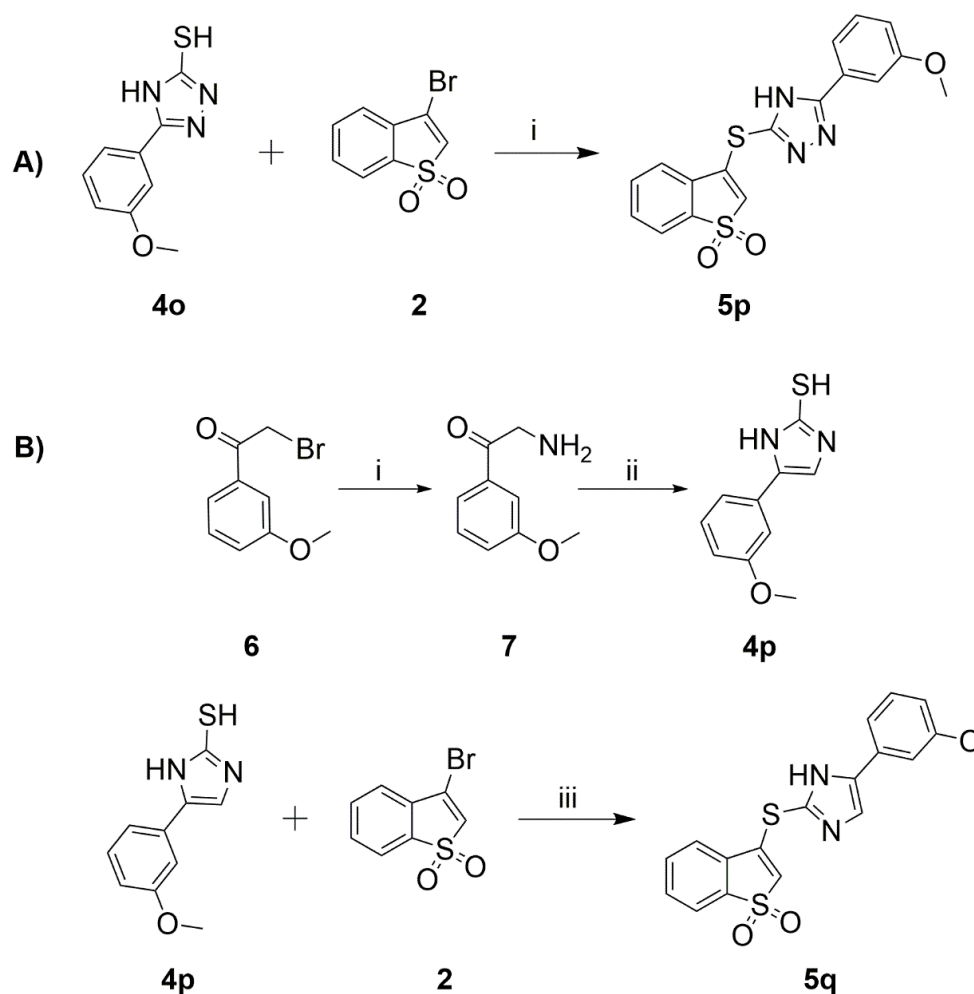
Scheme 2. Synthetic route of final compounds. Reagents and conditions: i) CS$_2$, DMF, 70 °C, 6 h. ii) **2**, CuI, BtH, potassium *tert*-butoxide, 1,4-dioxane, 95 °C. *Reagents and conditions for **4e:** KOH, CS$_2$, ethanol, 70 °C, overnight; 2M HCl, pH 5.

[†]**4m** and **4n** were purchased from Chem-Impex International Inc.

Analogs of **5k** where the 1,3,4-oxadiazole ring was altered to 1,2,4 triazole (**5p**) and *1H*-imidazole (**5q**) were prepared according to the procedure outlined in **Scheme 3**. Compound **5p** was synthesized by coupling of commercially purchased thiol **4o** with intermediate 3-bromo benzo[*b*]thiophene 1,1-dioxide (**2**). Compound **5q** was synthesized in a three-step reaction that involved the initial conversion of 2-bromo-1-(3-methoxyphenyl)ethan-1-one (**6**) to 2-amino-1-(3-methoxyphenyl)ethan-1-one (**7**) using Delepine reaction conditions. In the second step, the corresponding thiol **4p** was obtained by the treatment of compound **7** with potassium thiocyanate and glacial acetic acid at 140 °C for 2 h. Finally, the thiol **4p** was coupled with the intermediate 3-bromo benzo[*b*]thiophene 1,1-dioxide (**2**) to give **5q**.

7

Scheme 3. A) Synthetic route of compound **5p**. Reagents and conditions: i) CuI, BtH, potassium *tert*-butoxide, 1,4-dioxane, 95 °C; B) synthetic route of compound **5q**. Reagents and conditions: i) hexamine, DCM, rt, overnight; MeOH, HCl, 60 °C, 2h; ii) KSCN, glacial acetic acid, 140 °C, 2 h; iii) CuI, BtH, potassium *tert*-butoxide, 1,4-dioxane, 95 °C.

2.2. Biological screening

The designed compounds **5a-5o** were initially tested for their inhibitory activity against *Cryptococcus* IMPDH in an enzymatic assay, with MPA as a positive control. MPA showed *Cryptococcus* IMPDH inhibitory activity with an IC$_{50}$ of 0.12 ± 0.02 μM. All compounds, except compound **5l**, exhibited high inhibitory activity on *Cryptococcus* IMPDH with IC$_{50}$ values of ≤1 μM (**Table 1**). The relatively similar IC$_{50}$ values of all compounds against

8

Cryptococcus IMPDH suggested that any substitution made at the fifth position of the 1,3,4-oxadiazole ring did not influence the level of *Cryptococcus* IMPDH inhibition. Given the level of similarity between *Cryptococcus* IMPDH and the human IMPDH isoforms, it was also important to assess the selectivity of the compounds. Therefore, all compounds were also tested for inhibitory activity against the human IMPDH isoforms I and II. Interestingly, compounds **5f** and **5l** with 4-methyl carboxylate phenyl and 4-methoxy phenyl, respectively, at the fifth position of the 1,3,4-oxadiazole ring showed higher inhibitory selectivity (>30-fold) for *Cryptococcus* IMPDH (**5f** = 0.34 ± 0.07 μM, **5l** = 1.7 ± 0.38 μM) over the human IMPDH I and II isoforms (**5f** and **5l** = 30 μM).
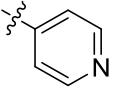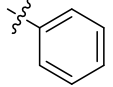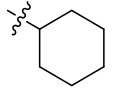
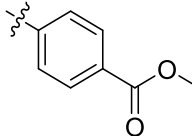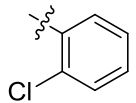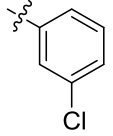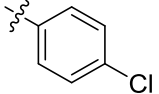Since IMPDH is evolutionarily conserved, these compounds might also inhibit other pathogenic fungi such as *C. albicans* and *A. fumigatus*. As an initial effort we tested the synthesized compounds at cellular level against *C. neoformans* (type strain H99; ATCC 208821) along with *C. albicans* (ATCC 90028), in order to evaluate their potential as broad-spectrum antifungal agents. The in vitro antifungal screening was performed at a concentration range of 256 μg/mL to 0.12 μg/mL. We observed that compounds **5a-5d** exhibited good inhibition against *C. neoformans* and *C. albicans* with MIC values ranging from 4 to 9 μM. Most of the other compounds showed prominent antifungal activity against *C. neoformans* but not *C. albicans*. These fungi have very different cellular structure for example *C. neoformans* has a polysaccharide capsule absent in *C. albicans* and this may alter the compound ability to penetrate the cell and subsequently inhibit IMPDH.
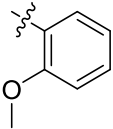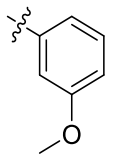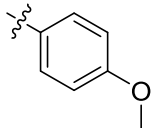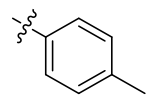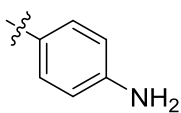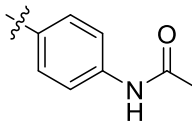
Finally, the cytotoxicity of **5a-5o** was tested using human embryonic kidney 293 (HEK293) and human liver hepatocellular carcinoma (HepG2) cell lines, with Tamoxifen as the positive control. All of these compounds displayed potent cytotoxic activity against the tested cell lines,

9

with CC_{50} values in the range of 2-6 μM for the HEK293 cell line and 14-31 μM for HepG2 cell line (**Table 1**). Our attempts to reduce the cytotoxicity by the modification of the 1,3,4-oxadiazole ring to 1,2,4 triazole in compound **5p** and 1*H*-imidazole in compound **5q** decreased *Cryptococcus* IMPDH inhibitory activity (**5p**: 14.6 ± 1.4 μM; **5q**: 24.3 ± 3 μM) and antifungal activity (**5p** and **5q** >172 μM) against both *C. neoformans* and *C. albicans*. This suggested that the 1,3,4-oxadiazole moiety was important for *Cryptococcus* IMPDH inhibitory activity but also lead to cytotoxicity. As IMPDH functions biologically as a homotetramer, with each monomer consisting of the active site for binding the substrate IMP and the cofactor NAD, the two most probable ways to inhibit IMPDH would be through binding to the active site or at subunit homotetrameric interfaces.

Table 1: Biological activities of 3-((5-substituted)-1,3,4-oxadiazol-2-yl)thio)benzo[*b*]thiophene 1,1-dioxide derivatives.
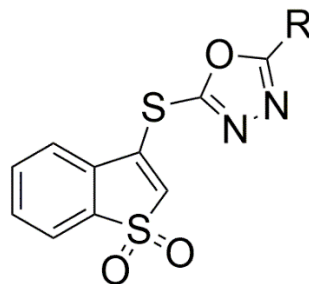
Compound	R	IMPDH inhibition (IC$_{50}$)[a] (µM)			Antifungal activity (MIC)[b] (µM)		Cytotoxicity (CC$_{50}$)[c] (µM)	
		Cryptococcus IMPDH	Human IMPDH I	Human IMPDH II	*C. neoformans*	*C. albicans*	HEK293	HepG2
MPA	-	0.12 ± 0.02	0.26 ± 0.01	0.11 ± 0.01	-	-	-	-
Amphotericin B	-	-	-	-	0.25	0.18	-	-
Fluconazole	-	-	-	-	0.3	8	-	-
Tamoxifen	-	-	-	-	-	-	39.4	24.7
5a		1.06 ± 0.03	13.2 ± 0.6	4.2 ± 0.6	6	4	5	24
5b		0.59 ± 0.14	6.3 ± 1	2.6 ± 0.4	4	4	4	14

11

	Structure						
5c		0.76 ± 0.07	8.6 ± 1	2.1 ± 0.2	9	6	4	17
5d		0.37 ± 0.06	5.6 ± 1	2.1 ± 0.1	6	6	3	20
5e		0.67 ± 0.16	7.6 ± 0.2	2.2 ± 0.7	7	46	3	15
5f		0.34 ± 0.07	>30	>30	60	>160	4	18
5g		0.23 ± 0.05	7.2 ± 1	1.2 ± 0.5	6	167	4	25
5h		0.40 ± 0.19	10.1 ± 3.4	1.6 ± 0.7	6	167	6	27
5i		0.49 ± 0.23	11.1 ± 3.6	1.5 ± 0.5	16	167	3	22

12

5j		0.48 ± 0.10	9.9 ± 0.6	3.2 ± 1	64	172	3	16
5k		0.15 ± 0.05	4.3 ± 0.4	1.2 ± 0.2	8	172	3	20
5l		1.7 ± 0.38	>30	>30	172	172	2	22
5m		0.41 ± 0.06	20.3 ± 1.4	5.7 ± 0.6	22	90	3	31
5n		1.01 ± 0.14	13.8 ± 0.6	4.5 ± 0.1	33	>179	4	24
5o		0.16 ± 0.05	20.4 ± 1.6	4.4 ± 0.6	>160	>160	4	31

[a]IC$_{50}$ values of the compounds against *Cryptococcus* IMPDH and human IMPDH isoforms I and II. The values represent the average of at least three independent experiments and include standard deviations.

13

[b]Antifungal assays were carried out in duplicate with DMSO as the negative control, whereas amphotericin B and fluconazole were used as positive controls.

[c]Cytotoxic activities of the compounds with DMSO as the negative control and tamoxifen as the positive control

14

2.3. Enzyme inhibition kinetics

To further understand the mechanism of enzyme inhibition, a Michaelis-Menten enzyme kinetic analysis was performed. Initial experiments to determine the Michaelis constant (K_m) were undertaken using the assay conditions [buffer containing 50 mM Tris-HCl (pH 8.0), 100 mM KCl, 3 mM EDTA, 1 mM DTT] reported by Morrow et al. for their kinetic studies.[12] Similar to all other IMPDHs, *Cryptococcus* IMPDH also exhibited substrate inhibition at higher concentrations of NAD.[11,12,21-24] Therefore, the K_m value of NAD ($K_{m(NAD)} = 402 \pm 91$ µM) was calculated by fitting kinetic data to a modified Michaelis-Menten equation that takes substrate inhibition into account (Equation 5). The apparent K_m value of IMP ($K_{m(IMP)} = 94 \pm 18$ µM) was determined with sub-saturating concentrations of NAD (700 µM) due to substrate inhibition and fitted into the classical Michaelis-Menten equation (Equation 4). The inhibition kinetics were also performed with MPA and compounds **5d** and **5j** by varying the concentration of one substrate, while the other substrate was maintained at a fixed concentration (**Table 2**). Consistent with previous reports, MPA showed uncompetitive inhibition (both V_{max} and K_m decreased) against both substrates, because it binds at the NAD site of the enzyme-substrate covalent complex (E-XMP*) formed after NADH leaves in the first step of the enzymatic reaction.[11]

Initially, there was no inhibitory activity observed for compounds **5d** and **5j** when tested in the DTT-containing buffer, which was used to determine the K_m values for the substrates. To investigate this, liquid chromatography-mass spectrometry (LC-MS) analysis of samples with compounds **5a**-**5o** dissolved in a DTT-containing buffer was employed and showed their breakdown due to the attack of the free thiol group of DTT at the C3-position of the benzo[*b*]thiophene 1,1-dioxide moiety; 5-substituted-1,3,4-oxadiazole thiols were detected in the mass spectra (**Figure 2**).
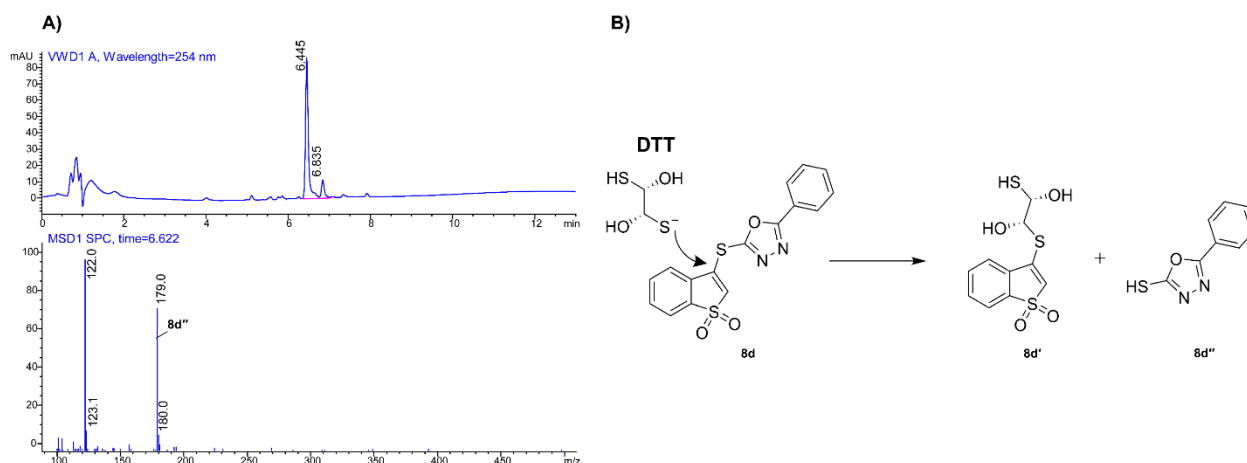
Figure 2. A) LC-MS of compound **5d** in buffer containing DTT. B) Mechanism of breakdown of compound **5d** by the attack of a free thiol of DTT at the C3-position of benzo[*b*]thiophene 1,1-dioxide.

The degradation of the benzo[*b*]thiophene 1,1-dioxide moiety supported the recent findings of Dahlin et al.,[13] who reported that the compounds with this chemotype as PAINS that formed covalent adducts when treated with glutathione (GSH); these adducts were detected using mass spectrometry (MS). Thus, inhibition kinetics for compounds **5d** and **5j** were performed using a buffer without DTT, and with different concentrations of one substrate and fixed concentrations of the other, with inhibitor concentrations from 0 to 20 µM. The plots obtained with the best fit of kinetic data from both compounds showed a decrease in the V_{max} value and increase in the K_m value (**Figure 3 and Table 2**). However, based on our studies (with DTT) and the observed thiol reactivity of these compounds,[13] it could be possible that free thiol groups of cysteine residues of other proteins, including *Cryptococcus* IMPDH, could be modified. *Cryptococcus* IMPDH has a cysteine residue in the active site that makes a covalent interaction with IMP during initial step of biological catalysis, as well as other free cysteines. To confirm that the inhibitory activity shown by synthesized compounds was due to the modification of cysteine residues in IMPDH we performed MS studies.

16
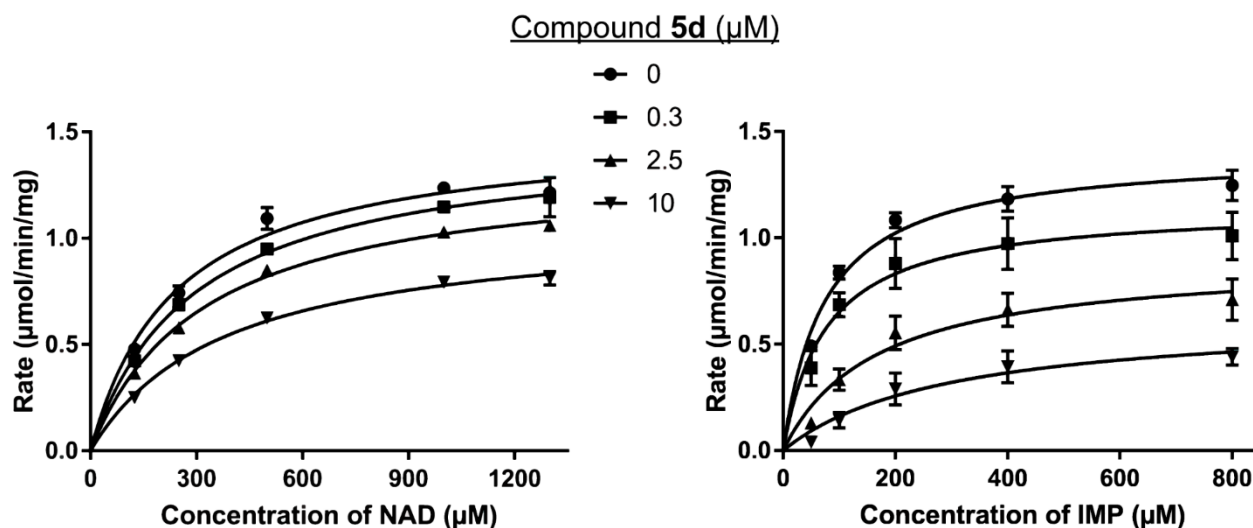
Figure 3. Inhibition kinetics at different concentrations of compound **5d** in conditions: A) by varying the concentration of NAD, while holding IMP at a fixed concentration (500 µM) B) by varying the concentration of IMP, while holding NAD at a fixed concentration (700 µM). The data were fitted to Equation 4 shown in experimental section.

17

Table 2: Kinetic parameters for *Cryptococcus* IMPDH reaction and inhibition by compounds **5d** and **5j**. The concentrations of fixed substrate are 500 µM for IMP and 700 µM for NAD, with NAD concentration varied from 31.25 µM to 1300 µM and IMP from 25 µM to 800 µM. The data were fitted to Equation 4 shown in experimental section.

Substrate			Inhibition kinetics									
Fixed	Varied	Kinetic parameters	No inhibitor	MPA (µM)			5d (µM)			5j (µM)		
				0.039	0.078	0.156	0.3	2.5	10	0.3	2.5	10
IMP	NAD	V_{max} (µM/min)	1.5	1.1	0.6	0.26	1.5	1.3	1	1.5	1.5	1
		K_m (µM)	257.5 ± 23	200 ± 15	137 ± 12	37	307 ± 22	336 ± 17	386 ± 23	278 ± 21.5	358.5 ± 36	355 ± 20
		K_{cat} (s⁻¹)	1.5	1.1	0.6	0.25	1.5	1.3	1	1.5	1.5	1
NAD	IMP	V_{max} (µM/min)	1.45	0.9	0.6	0.3	1.1	0.9	0.6	1.4	1	0.7
		K_m (µM)	90 ± 12	64 ± 13	53 ± 10	32 ± 7.5	92.5 ± 19	187 ± 44	315.5 ± 95	93 ± 11	165 ± 26	258 ± 47
		K_{cat} (s⁻¹)	1.38	0.9	0.6	0.3	1.1	0.9	0.6	1.4	1	0.7

18

2.4. Mass spectrometry studies

Intact MS studies were conducted for samples of His-tagged *Cryptococcus* IMPDH in the absence and presence of compound **5d**. Deconvoluted MS data showed that the intact mass of His-tagged *Cryptococcus* IMPDH as 59308 Da (theoretical mass = 59289 Da), and His-tagged *Cryptococcus* IMPDH incubated with compound **5d** were determined as 59471 Da, 59633 Da and 59794 Da, which corresponded to single, double and triple modifications of cysteine residues from the addition of 164 Da (from attack of a thiol group in cysteine at the C3-position of benzo[*b*]thiophene 1,1-dioxide of **5d**) (**Figure 4**). To investigate and characterize the modification of cysteine residues and confirm sites of cysteine modification in the sequence of *Cryptococcus* IMPDH, our mass spectrometry studies were extended to peptide sequencing.
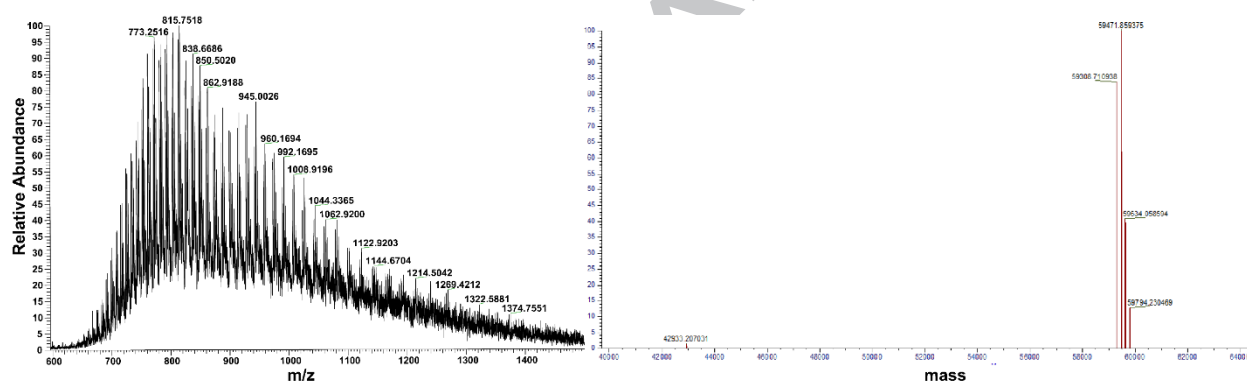
Figure 4. A) Mass spectrometry of His-tagged *Cryptococcus* IMPDH incubated with compound **5d**. B) The deconvoluted mass spectrum showing intact masses of unmodified (59308.71 Da) and modified protein (59471.85 Da, 59634 Da and 59794.23 Da).

The PeptideMass tool on the Expasy server[25,26] predicted 35 tryptic peptide fragments generated from IMPDH, with the seven cysteines in seven unique peptides (**Table S1**). The catalytic cysteine (Cys 357) is present in fragment 5 (residue 349-382, M = 3455.7046 Da), which corresponded to the active site loop in *Cryptococcus* IMPDH. The fragments identified from the His-tagged *Cryptococcus* IMPDH sample showed good coverage of 97% with 95% confidence. The peptide fragment 5 produced an ion at *m/z* 1153.9 [(M + 3H)$^{3+}$], which agreed

with the theoretical *m/z* value for 3+ protonated peptide (**Figure S1**). All cysteine containing peptide fragments were also detected by the database search (**Figure S3-S7**).

Tryptic digestion of His-tagged *Cryptococcus* IMPDH incubated with compound **5d** on ice and room temperature resulted in 81% coverage (at a 95% confidence) of the protein sequence and modification of 5 cysteines with the 164 Da from benzo[*b*]thiophene 1,1-dioxide from compound **5d** (**Figure S2** and **S8-S11**). This was consistent with the multiple modifications observed in the mass spectra of the undigested His-tagged *Cryptococcus* IMPDH incubated with compound **5d**. Interestingly, the catalytic cysteine (Cys 357) containing peptide fragment 5 (residues 349-382) was not detected in this sample, neither in the unmodified or modified form. Some differences with the enzyme-only digest were also detected, where peptide fragment 1 (residue 108-135) was found as a mis-cleaved form containing residues 125-135, with cyano group modification on cysteine.

3. Conclusions

3-((5-Substituted)-1,3,4-oxadiazol-2-yl)thio)benzo[*b*]thiophene 1,1-dioxides identified by high-throughput screening of *Cryptococcus* IMPDH were investigated as potential antifungals. All analogs **5a**-**5o** had similar *Cryptococcus* IMPDH *in vitro* activities (≤ 1 µM) but exhibited potent human cell line cytotoxicities. Modifications to the 1,3,4-oxadiazole ring led to decreased cytotoxicity but also impaired *Cryptococcus* IMPDH inhibition and antifungal activities. The inhibition kinetics of compounds **5d** and **5j** using previously reported conditions that incorporated DTT did not show *Cryptococcus* IMPDH inhibitory activity due to the adduct formation of the benzo[*b*]thiophene 1,1-dioxide with DTT. Further investigation through MS studies confirmed that these compounds made covalent bound to multiple cysteine residues in *Cryptococcus* IMPDH in a promiscuous fashion. This reinforces the importance of eliminating PAINS from screening libraries.

20

4. Experimental section

4.1. Chemistry

4.1.1. General Methods and Materials

All starting materials were purchased from standard commercial sources and used without further purification, unless otherwise stated. All reactions were carried out with magnetic stirring using magnetic bars under an inert nitrogen atmosphere with anhydrous solvents unless otherwise stated. The progress of reactions was monitored by either thin-layer chromatography (TLC) on 0.25 mm silica gel plates (TLC) on 0.25 mm silica gel plates (60F-254) and visualized with UV light or a $KMnO_4$ dip. Analytical ^1H and ^{13}C NMR spectra were recorded in deuterated solvents at 298 K on a Varian Unity 400 MHz or Bruker Advance 600 MHz spectrometers. The chemical shifts are reported as a part per million (ppm) downfield from tetramethylsilane (TMS) and coupling constants (*J*) were calculated in hertz (Hz). All final compounds were purified to ≥95% by the Grace Reveleris chromatography instrument using UV detection. High resolution mass spectrometry (HRMS) was performed on the Bruker MicroTOF mass spectrometer.

4.1.2. General procedure for synthesis of 5-substituted 1,3,4-oxadiazole-2-thiols

To a solution of acid hydrazide in anhydrous 5-15 mL of DMF, carbon disulfide (2.5 mL/mmol) was added at room temperature and under a nitrogen atmosphere. The reaction mixture was then heated to 40 °C for 15 minutes and then to 70 °C for 4-8 h until the reaction was completed. After completion, the reaction mixture was cooled to room temperature and poured dropwise into ice cold water. The solids formed were separated by filtration, washed with water and dried *in vacuo*.

5-(Pyridin-2-yl)-1,3,4-oxadiazole-2-thiol (4a) Prepared from pyridine-2-carbohydrazide **3a** (0.3 g, 21.8 mmol) and CS_2 (0.5 g, 6.50 mmol) according to general procedure A. Yield 170

mg (43%); yellow solid; MS (ESI) *m/z* (%): 180.2 [M+H]$^+$. ^{1}H NMR (400 MHz, DMSO-d_6) δ 14.8 (s, 1H), 8.76 (dd, *J* = 1.7, 1.1 Hz, 1H), 8.09-7.97 (m, 2H), 7.64 (dd, *J* = 4.8, 1.9 Hz, 1H).

5-(Pyridin-3-yl)-1,3,4-oxadiazole-2-thiol (**4b**) Prepared from pyridine-3-carbohydrazide **3b** (0.3 g, 21.8 mmol) and CS$_2$ (0.5 g, 6.50 mmol) according to general procedure A. Yield 120 mg (30%); yellow solid; MS (ESI) *m/z* (%): 180.2 [M+H]$^+$. ^{1}H NMR (400 MHz, DMSO-d_6) δ 9.04 (dd, J = 2.3, 0.9 Hz, 1H), 8.79 (dd, J = 4.9, 1.6 Hz, 1H), 8.31-8.20 (m, 1H), 7.68-7.54 (m, 1H).

5-(Pyridin-4-yl)-1,3,4-oxadiazole-2-thiol (4c) Prepared from pyridine-4-carbohydrazide **3c** (0.3 g, 21.8 mmol) and CS$_2$ (0.5 g, 6.50 mmol) according to general procedure A. Yield 180 mg (50%); yellow solid; MS (ESI) *m/z* (%): 180.2 [M+H]$^+$. ^{1}H NMR (400 MHz, DMSO-d_6) δ 9.05-8.92 (m, 2H), 8.09 - 7.97 (m, 2H).

5-(Phenyl)-1,3,4-oxadiazole-2-thiol (4d) Prepared from benzohydrazide **3d** (1.0 g, 5.6 mmol) and CS$_2$ (1.6 g, 21.0 mmol) according to general procedure A. Yield 0.52 g (40%); yellow solid; MS (ESI) *m/z* (%): 179.2 [M+H]$^+$. ^{1}H NMR (400 MHz, DMSO-d_6) δ 14.7 (s, 1H), 7.93-7.85 (m, 2H), 7.69-7.55 (m, 2H).

Methyl 4-(5-mercapto-1,3,4-oxadiazol-2-yl)benzoate (4f) Prepared from methyl 4-(hydrazinecarbonyl)benzoate **3f** (0.15 g, 0.77 mmol) and CS$_2$ (0.12 g, 1.50 mmol) according to general procedure A. Yield 120 mg (66%); yellow solid; MS (ESI) *m/z* (%): 237.2 [M+H]$^+$. ^{1}H NMR (400 MHz, DMSO-d_6) δ 10.79 (s, 1H), 8.15- 8.09 (m, 2H), 8.06-8.00 (m, 2H), 3.90 (d, *J* = 1.4 Hz, 3H).

5-(2-Chlorophenyl)-1,3,4-oxadiazole-2-thiol (4g) Prepared from 2-chlorobenzohydrazide **3g** (2.0 g, 11.7 mmol) and CS$_2$ (2.6 g, 34.2 mmol) according to general procedure A. Yield 1.53 g (63%); yellow solid; MS (ESI) *m/z* (%): 213.3 [M+H]$^+$. ^{1}H NMR (400 MHz, DMSO-d_6) δ 7.88 (ddd, *J* = 7.8, 1.7, 0.5 Hz, 1H), 7.67 (dd, *J* = 1.4, 0.5 Hz, 1H), 7.61 (dd, *J* = 1.4, 0.5 Hz, 1H), 7.52 (dd, *J* = 1.4, 0.5 Hz, 1H).

22

5-(3-Chlorophenyl)-1,3,4-oxadiazole-2-thiol (4h) Prepared from 3-chlorobenzohydrazide **3h** (2.0 g, 11.7 mmol) and CS_2 (2.6 g, 34.2 mmol) according to general procedure A. Yield 1.4 g (58%); yellow solid; MS (ESI) *m/z* (%): 213.3 [M+H]$^+$. ^{1}H NMR (400 MHz, DMSO-d_6) δ 14.79 (s, 1H), 7.84-7.80 (m, 1H), 7.80 (dd, J = 1.6, 1.1 Hz, 1H), 7.67 (dd, J = 2.1, 1.1 Hz, 1H), 7.58 (dd, J = 1.6, 0.6 Hz, 1H).

5-(4-Chlorophenyl)-1,3,4-oxadiazole-2-thiol (4i) Prepared from 4-chlorobenzohydrazide **3i** (2.0 g, 11.7 mmol) and CS_2 (2.6 g, 34.2 mmol) according to general procedure A. Yield 1.4 g (58%); yellow solid; MS (ESI) *m/z* (%): 213.3 [M+H]$^+$. ^{1}H NMR (400 MHz, DMSO-d_6) δ 7.94-7.81 (m, 2H), 7.67 - 7.58 (m, 2H).

5-(2-Methoxyphenyl)-1,3,4-oxadiazole-2-thiol **(4j)** Prepared from 2-methoxybenzohydrazide **3j** (2.0 g, 12.0 mmol) and CS_2 (2.74 g, 36.0 mmol) according to general procedure A. Yield 1.7 g (68%); yellow solid; MS (ESI) *m/z* (%): 209.2 [M+H]$^+$. ^{1}H NMR (400 MHz, DMSO-d_6) δ 7.70 (dd, *J* = 7.7, 1.8 Hz, 1H), 7.62-7.48 (m, 1H), 7.22 (dd, *J* = 8.5, 0.9 Hz, 1H), 7.08 (td, *J* = 7.5, 0.9 Hz, 1H), 3.86 (s, 3H).

5-(3-Methoxyphenyl)-1,3,4-oxadiazole-2-thiol **(4k)** Prepared from 3-methoxybenzohydrazide **3k** (2.0 g, 12.0 mmol) and CS_2 (2.74 g, 36.0 mmol) according to general procedure A. Yield 1.6 g (64%); yellow solid; MS (ESI) *m/z* (%): 209.2 [M+H]$^+$. ^{1}H NMR (400 MHz, DMSO-d_6) δ 7.50-7.41 (m, 2H), 7.31 (dd, *J* = 1.5, 0.4 Hz, 1H), 7.17 (dd, *J* = 2.7, 1.3 Hz, 1H), 3.81 (s, 3H).

5-(4-Methoxyphenyl)-1,3,4-oxadiazole-2-thiol **(4l)** Prepared from 4-methoxybenzohydrazide **3l** (2.0 g, 12.0 mmol) and CS_2 (2.74 g, 36.0 mmol) according to general procedure A. Yield 1.5 g (60%); yellow solid; MS (ESI) *m/z* (%): 209.2 [M+H]$^+$. ^{1}H NMR (400 MHz, DMSO-d_6) δ 7.83-7.74 (m, 2H), 7.17-7.05 (m, 2H), 3.81 (s, 3H).

Synthesis of 5-(Cyclohexyl)-1,3,4-oxadiazole-2-thiol (**4e**) To solution of synthesized cyclohexyl hydrazide **3e** (0.5 g, 3.52 mmol) in ethanol, potassium hydroxide (0.25 g, 4.46

23

mmol) and carbon disulfide (1.3 g, 17.1mmol) were added at room temperature and under a nitrogen atmosphere. The reaction mixture was then heated to 70 °C overnight. The reaction mixture was evaporated *in vacuo* and acidified to pH 5 with 2 M HCl. The aqueous layer was extracted with ethyl acetate (3×50 mL) and organics were dried (MgSO$_4$) and concentrated *in vacuo* to yield 5-(cyclohexyl)-1,3,4- oxadiazole-2-thiol (**4e**) as colorless oil; yield 0.25 mg (39%) MS (ESI) *m/z* (%): 185.1 [M+H]$^+$. ^{1}H NMR (400 MHz, DMSO-d_6) δ 2.77 (tt, *J* = 10.9, 3.7 Hz, 1H), 1.94-1.87 (m, 2H), 1.71-1.55 (m, 3H), 1.45-1.16 (m, 5H).

4.1.3. Synthesis of 5-(3-Methoxyphenyl)-1*H*-imidazole-2-thiol (4p)

Step A. To a solution of 2-bromo-1-(3-methoxyphenyl)ethan-1-one) (2.0 g, 8.70 mmol) in 20 mL of dichloromethane, hexamine (1.46 g, 10.4 mmol) was added and the mixture was stirred at room temperature overnight. The white solids formed were separated by filtration and dried *in vacuo*. Then solids were dissolved in 15 mL of methanol and 2 mL of c. HCl and heated at 60 °C for 3 h. The reaction completion was monitored by LC-MS and then reaction mixture was cooled and filtered to separate the inorganics. Excess solvent from the filtrate was evaporated *in vacuo* and solids were neutralized with aqueous solution of sat. NaHCO$_3$, separated by filtration and dried *in vacuo* to give 2-amino-1-(3-methoxyphenyl)ethan-1-one as a dark brown solid. Yield: 0.8 g, 57%; MS (ESI) *m/z* (%): 166.2 [M+H]$^+$. ^{1}H NMR (400 MHz, DMSO-d_6) δ 7.58 (dt, *J* = 7.8, 1.2 Hz, 1H), 7.51 – 7.45 (m, 2H), 7.27 (dd, *J* = 2.6, 0.9 Hz, 1H), 4.55 (s, 2H), 3.81 (s, 3H).

Step B. To a solution of 2-amino-1-(3-methoxyphenyl)ethan-1-one (0.2 g, 1.21 mmol) in 4 mL of glacial acetic acid, potassium thiocyanate (0.15g, 1.57 mmol) was added at room temperature and heated to 140 °C for 2 h. The reaction mixture was then diluted with water (25 mL) and extracted with ethyl acetate 2×50 mL. The organics were dried (MgSO$_4$) and evaporated *in vacuo* to give 5-(3-methoxyphenyl)-4H-1,2,4-triazole-3-thiol (**4p**) as a dark brown solid. Yield: 70 mg, 29%; MS (ESI) *m/z* (%): 207.2 [M+H]$^+$. ^{1}H NMR (400 MHz,

24

DMSO-d_6) δ 12.47 (s, 1H), 12.09 (s, 1H), 7.38 (t, J = 2.3 Hz, 1H), 7.28 - 7.18 (m, 3H), 6.78 (dd, J = 2.5, 1.6 Hz, 1H), 3.74 (s, 3H).

4.1.4. Synthesis of 3-bromobenzo[*b*]thiophene 1,1-dioxide (2)

To solution of **1** (1.0 g, 4.70 mmol) in dichloromethane, mCPBA (4.4 g, 25.0 mmol) was added at 0 °C and the mixture was warmed to room temperature and left stirring for 24 h. TLC was spotted with a small aliquot of the reaction mixture, which indicated that the reaction was completed. Excess DCM was added and washed with sat. $NaHCO_3$ (aq) (50 mL × 2), followed by brine solution (50 mL × 1). The organics were dried ($MgSO_4$) and evaporated in *vacuo*. The residue was then recrystallized from absolute ethanol to get product in good yield. White crystalline solid; Yield: 0.65 mg, 57%; MS (ESI) *m/z* (%): 247 [M+H]$^+$; ^{1}H NMR (400 MHz, $CDCl_3$) δ 7.76-7.53 (m, 4H), 6.98 (s, 1H).

4.1.5. General procedure for coupling of 3-bromobenzo[*b*]thiophene 1,1-dioxide with 5-substituted 1,3,4-oxadiazole-2-thiols

To a solution of 3-bromobenzo[*b*]thiophene 1,1-dioxide 2 dissolved in 1,4-dioxane (5 mL/mmol), CuI (0.5 mol %) and benzotriazole (1.0 mol %) were added and the mixture was stirred for 10 min at room temperature. Then thiols **4a**-**4p** and potassium *tert*-butoxide (1.5 eq) were added to the reaction mixture, which was stirred at 95 °C overnight. The reaction completion was monitored by LC-MS analysis. Then reaction mixture was cooled to room temperature and excess solvent was evaporated in *vacuo*. The residue obtained was dissolved in DMSO/acetonitrile (3:1) and loaded onto C18 column (GRACE Flash) for purification using water/acetonitrile as the mobile phase. The fractions that contained product were collected and lyophilized to provide 4a-4q in good yields.

3-((5-(Pyridin-2-yl)-1,3,4-oxadiazol-2-yl)thio)benzo[*b*]thiophene 1,1-dioxide (5a) Prepared from thiol **4a** (50.0 mg, 0.28 mmol) and **2** (82 mg, 0.33 mmol) according to general procedure E. Yield 16 mg (17%); light yellow solid; MS (ESI) *m/z* (%): 344.1 [M+H]$^+$. ^{1}H NMR (600

25

MHz, DMSO-d_6) δ 8.82 (ddd, J = 4.8, 1.7, 0.9 Hz, 1H), 8.25 (dt, J = 7.9, 1.1 Hz, 1H), 8.10 (td, J = 7.8, 1.8 Hz, 1H), 8.02-7.99 (m, 1H), 7.84-7.80 (m, 1H), 7.79-7.75 (m, 2H), 7.73 (s, 1H), 7.69 (dd, J = 4.8, 1.2 Hz, 1H). ^{13}C NMR (150 MHz, DMSO-d_6) δ 167.1, 157.6, 150.8, 142.9, 138.7, 138.4, 136.8, 135.0 ,132.5, 129.4, 127.3, 127.0, 123.8, 123.3, 121.8; HRMS calculated for $C_{15}H_{10}N_3O_3S_2$: 344.0158, found 344.0153.

3-((5-(Pyridin-3-yl)-1,3,4-oxadiazol-2-yl)thio)benzo[*b*]thiophene 1,1-dioxide (5b) Prepared from thiol **4b** (50.0 mg, 0.28 mmol) and **2** (82 mg, 0.33 mmol) according to general procedure E. Yield 14 mg (15%); light yellow solid; MS (ESI) *m/z* (%): 344.1 [M+H]+. ^{1}H NMR (600 MHz, DMSO-d_6) δ 9.22 (d, J = 2.1 Hz, 1H), 8.86 (dd, J = 5.0, 1.6 Hz, 1H), 8.43 (dt, J = 8.0, 2.0 Hz, 1H), 8.00 (d, J = 7.4 Hz, 1H), 7.85-7.74 (m, 4H), 7.69 (dd, J = 8.0, 5.0 Hz, 1H). ^{13}C NMR (150 MHz, DMSO-*d6*) δ 166.2, 157.3, 153.4, 147.9, 138.7, 136.8, 135.0, 134.9, 132.5, 129.4, 126.9, 124.8, 123.3, 121.8, 120.2; HRMS calculated for $C_{15}H_{10}N_3O_3S_2$: 344.0158, found 344.0164.

3-((5-(Pyridin-4-yl)-1,3,4-oxadiazol-2-yl)thio)benzo[*b*]thiophene 1,1-dioxide (5c) Prepared from thiol **4c** (50.0 mg, 0.28 mmol) and **2** (82 mg, 0.33 mmol) according to general procedure E. Yield 12 mg (13%); light yellow solid; MS (ESI) *m/z* (%): 344.1 [M+H]+. ^{1}H NMR (600 MHz, DMSO-d_6) δ 8.89 - 8.86 (m, 2H), 8.01 (t, J = 0.9 Hz, 1H), 7.99-7.98 (m, 2H), 7.84-7.75 (m, 4H). ^{13}C NMR (150 MHz, DMSO-d_6) δ 166.3, 158.0, 151.4, 138.51, 136.8, 134.9, 132.5, 130.6, 129.4, 127.1, 123.4, 121.8, 120.8; HRMS calculated for $C_{15}H_{10}N_3O_3S_2$: 344.0158, found 344.0168.

3-((5-Phenyl-1,3,4-oxadiazol-2-yl)thio)benzo[*b*]thiophene 1,1-dioxide (5d) Prepared from thiol **4d** (50.0 mg, 0.28 mmol) and **2** (82 mg, 0.33 mmol) according to general procedure E. Yield 35 mg (37%); light yellow solid; MS (ESI) *m/z* (%): 343.2 [M+H]+. ^{1}H NMR (600 MHz, DMSO-d_6) δ 8.06-8.04 (m, 2H), 8.00-7.96 (m, 1H) 7.83-7.80 (m, 1H), 7.78-7.74 (m, 3H), 7.70-7.67 (m, 1H), 7.65-7.62 (m, 2H). ^{13}C NMR (150 MHz, DMSO-d_6) δ 167.9, 156.6, 138.8, 136.8,

134.9, 133.0, 132.5, 129.9, 129.9, 129.4, 126.8, 123.5, 23.3, 121.8; HRMS calculated for $C_{16}H_{11}N_2O_3S_2$: 343.0205, found 343.0211.

3-((5-Cyclohexyl-1,3,4-oxadiazol-2-yl)thio)benzo[*b*]thiophene 1,1-dioxide (5e) Prepared from thiol **4e** (50.0 mg, 0.27 mmol) and 2 (79 mg, 0.32 mmol) according to general procedure E. Yield 18 mg (16%); light yellow solid; MS (ESI) *m/z* (%): 349.5 [M+H]$^+$. ^{1}H NMR (600 MHz, DMSO-*d$_6$*) δ 7.98 (dd, *J* = 7.5, 4.6 Hz, 1H), 7.82 - 7.74 (m, 2H), 7.70 (dd, *J* = 7.6, 4.6 Hz, 1H), 7.60 (d, *J* = 4.9 Hz, 1H), 3.04 (td, *J* = 11.1, 5.0 Hz, 1H), 2.06 - 2.01 (m, 2H), 1.74 (dt, *J* = 13.3, 4.3 Hz, 2H), 1.67-1.60 (m, 1H), 1.55 (q, *J* = 11.9 Hz, 2H), 1.43 - 1.34 (m, 2H), 1.27 (td, *J* = 12.2, 4.1 Hz, 1H). ^{13}C NMR (150 MHz, DMSO-*d$_6$*) δ 174.0, 156.4, 138.9, 137.1, 135.2, 132.8, 129.7, 127.1, 123.5, 122.1, 35.1, 30.00, 25.88, 25.3; HRMS calculated for $C_{16}H_{17}N_2O_3S_2$: 349.0675, found 349.0686.

Methyl 4-(5-((1,1-dioxidobenzo[*b*]thiophen-3-yl)thio)-1,3,4-oxadiazol-2-yl)benzoate (5f) Prepared from thiol **4f** (50.0 mg, 0.21 mmol) and **2** (61.0 mg, 0.25 mmol) according to general procedure E. Yield 5 mg (6%); light yellow solid; MS (ESI) *m/z* (%): 401.4 [M+H]$^+$. ^{1}H NMR (600 MHz, DMSO-*d$_6$*) δ 8.24-8.16 (m, 4H), 8.00 (dt, *J* = 7.5, 1.0 Hz, 1H), 7.87- 7.73 (m, 4H), 3.91 (s, 3H). ^{13}C NMR (150 MHz, DMSO-*d$_6$*) δ 167.2, 165.8, 157.3, 138.7, 136.8, 134.9, 133.1, 132.5, 130.6, 129.4, 127.8, 127.4, 126.9, 123.3, 121.8, 53.0; HRMS calculated for $C_{18}H_{13}N_2O_5S_2$: 401.0260, found 401.0260.

3-((5-(2-Chlorophenyl)-1,3,4-oxadiazol-2-yl)thio)benzo[*b*]thiophene 1,1-dioxide (5g) Prepared from thiol **4g** (50.0 mg, 0.23 mmol) and **2** (67 mg, 0.27 mmol) according to general procedure E. Yield 24 mg (32%); dark brown solid; MS (ESI) *m/z* (%): 377.2 [M+H]$^+$. ^{1}H NMR (600 MHz, DMSO-*d$_6$*) δ 8.07 (dd, *J* = 7.9, 1.7 Hz, 1H), 8.01 - 7.99 (m, 1H), 7.84 - 7.80 (m, 2H), 7.78 - 7.73 (m, 3H), 7.69 (dd, *J* = 7.4, 1.7 Hz, 1H), 7.62 - 7.59 (m, 1H). ^{13}C NMR (150 MHz, DMSO-*d$_6$*) δ 165.8, 157.5, 138.0, 136.8, 134.9, 134.1, 132.5, 132.3, 131.9, 131.7,

27

129.5, 128.3, 127.9, 123.4, 122.3, 121.8; HRMS calculated for $C_{16}H_{10}ClN_2O_3S_2$: 376.9816, found 376.9802

3-((5-(3-Chlorophenyl)-1,3,4-oxadiazol-2-yl)thio)benzo[*b*]thiophene 1,1-dioxide (5h)
Prepared from thiol **4h** (50.0 mg, 0.23 mmol) and **2** (67 mg, 0.27 mmol) according to general procedure E. Yield 26 mg (33%); dark brown solid; MS (ESI) *m/z* (%): 377.2 [M+H]⁺. ¹H NMR (600 MHz, DMSO-*d₆*) δ 8.06-7.99 (m, 3H), 7.84-7.81 (m, 1H), 7.79-7.75 (m, 4H), 7.68 (t, *J* = 8.0 Hz, 1H). ¹³C NMR (150 MHz, DMSO-*d₆*) δ 166.8, 157.2, 138.6, 136.8, 134.9, 134.5, 132.8, 132.5, 132.0, 129.4, 127.0, 126.8, 126.1, 125.4, 123.3, 121.8; HRMS calculated for $C_{16}H_{10}ClN_2O_3S_2$: 376.9816, found 376.9812.

3-((5-(4-Chlorophenyl)-1,3,4-oxadiazol-2-yl)thio)benzo[*b*]thiophene 1,1-dioxide (5i)
Prepared from thiol **4i** (50.0 mg, 0.23 mmol) and **2** (67.0 mg, 0.27 mmol) according to general procedure E. Yield 20 mg (26%); dark brown solid; MS (ESI) *m/z* (%): 377.2 [M+H]⁺. ¹H NMR (600 MHz, DMSO-*d₆*) δ 8.09-8.03 (m, 2H), 7.99 (dd, *J* = 7.1, 1.6 Hz, 1H), 7.83-7.74 (m, 4H), 7.73-7.70 (m, 2H). ¹³C NMR (150 MHz, DMSO-*d₆*) δ 167.2, 156.9, 138.7, 137.7, 136.8, 134.9, 132.5, 130.1, 129.4, 129.2, 126.8, 123.3,122.4, 121.8; HRMS calculated for $C_{16}H_{10}ClN_2O_3S_2$: 376.9816, found 376.9801.

3-((5-(2-Methoxyphenyl)-1,3,4-oxadiazol-2-yl)thio)benzo[*b*]thiophene 1,1-dioxide (5j)
Prepared from thiol **4j** (50.0 mg, 0.24 mmol) and 2 (67.0 mg, 0.28 mmol) according to general procedure E. Yield 18 mg (18%); light yellow solid; MS (ESI) *m/z* (%): 373.1 [M+H]⁺. ¹H NMR (600 MHz, DMSO-*d₆*) δ 8.00 (d, *J* = 7.4 Hz, 1H), 7.92 (dd, *J* = 7.9, 1.7 Hz, 1H), 7.81 (t, *J* = 7.5 Hz, 1H), 7.78-7.73 (m, 2H), 7.71 (s, 1H), 7.66-7.62 (m, 1H), 7.28 (d, *J* = 8.6 Hz, 1H), 7.16 (t, *J* = 7.6 Hz, 1H), 3.88 (s, 3H). ¹³C NMR (150 MHz, DMSO-*d₆*) δ 166.6, 157.9, 156.5, 138.3, 136.8, 134.9, 134.6, 132.5, 130.7, 127.4, 123.3, 123.3, 121.8, 121.2, 113.2, 112.0, 56.4; HRMS calculated for $C_{17}H_{13}N_2O_4S_2$: 373.0311, found 373.0309.

3-((5-(3-Methoxyphenyl)-1,3,4-oxadiazol-2-yl)thio)benzo[*b*]thiophene 1,1-dioxide (5k)

Prepared from thiol **4k** (50.0 mg, 0.24 mmol) and **2** (67.0 mg, 0.28 mmol) according to general procedure E. Yield 10 mg (10%); light yellow solid; MS (ESI) *m/z* (%): 373.1 [M+H]$^+$. ^{1}H NMR (600 MHz, DMSO-*d$_6$*) δ 7.99 (dd, *J* = 7.8, 1.2 Hz, 1H), 7.84-7.79 (m, 1H), 7.79-7.72 (m, 3H), 7.62 (dt, *J* = 7.7, 1.2 Hz, 1H), 7.55 (t, *J* = 8.0 Hz, 1H), 7.51 (dd, *J* = 2.7, 1.6 Hz, 1H), 7.26 (dd, *J* = 2.7, 1.0 Hz, 1H), 3.85 (s, 3H). ^{13}C NMR (150 MHz, DMSO-*d$_6$*) δ 167.6, 160.1, 156.8, 138.7, 136.8, 134.9, 132.5, 131.3, 129.4, 127.1, 124.6, 123.3, 121.8, 119.7, 119.0, 112.0, 55.9; HRMS calculated for $C_{17}H_{13}N_2O_4S_2$: 373.0294, found 373.0311.

3-((5-(4-Methoxyphenyl)-1,3,4-oxadiazol-2-yl)thio)benzo[*b*]thiophene 1,1-dioxide (5l)

Prepared from thiol **4l** (50.0 mg, 0.24 mmol) and **2** (67.0 mg, 0.28 mmol) according to general procedure E. Yield 15 mg (15%); light yellow solid; MS (ESI) *m/z* (%): 373.1 [M+H]$^+$. ^{1}H NMR (600 MHz, DMSO-*d$_6$*) δ 8.02-7.96 (m, 3H), 7.81 (td, *J* = 7.5, 1.2 Hz, 1H), 7.79-7.74 (m, 2H), 7.72 (s, 1H), 7.20-7.15 (m, 2H), 3.86 (s, 3H). ^{13}C NMR (150 MHz, DMSO-*d$_6$*) δ 167.8, 162.9, 155.7, 138.9, 136.8, 134.9, 132.5, 129.4, 129.3, 126.6, 123.2, 121.8, 115.7, 115.3, 56.0; HRMS calculated for $C_{17}H_{13}N_2O_4S_2$: 373.0311, found 373.0293.

3-((5-(p-Tolyl)-1,3,4-oxadiazol-2-yl)thio)benzo[*b*]thiophene 1,1-dioxide (5m) Prepared from thiol **4m** (50.0 mg, 0.25 mmol) and **2** (73.0 mg, 0.3 mmol) according to general procedure E. Yield 13 mg (18%); light yellow solid; MS (ESI) *m/z* (%): 157.4 [M+H]$^+$. ^{1}H NMR (600 MHz, DMSO-*d$_6$*) δ 8.01-7.99 (m, 1H), 7.94 (d, *J* = 8.2 Hz, 2H), 7.84- 7.80 (m, 1H), 7.79-7.75 (m, 2H), 7.74 (s, 1H), 7.45 (d, *J* = 8.0 Hz, 2H), 2.42 (s, 3H). ^{13}C NMR (150 MHz, DMSO-*d$_6$*) δ 168.0, 156.2, 143.3, 138.8, 136.8, 134.9, 132.5, 130.4, 129.4, 127.3, 126.8, 123.3, 121.8, 120.7, 21.6; HRMS calculated for $C_{17}H_{13}N_2O_3S_2$: 357.0362, found 357.0376.

3-((5-(4-Aminophenyl)-1,3,4-oxadiazol-2-yl)thio)benzo[*b*]thiophene 1,1-dioxide (5n)

Prepared from thiol **4n** (50.0 mg, 0.25 mmol) and **2** (73.0 mg, 0.3 mmol) according to general procedure E. Yield 30 mg (26%); Dark yellow solid; MS (ESI) *m/z* (%): 358.2 [M+H]$^+$. ^{1}H

NMR (600 MHz, DMSO-d_6) δ 7.98 (d, J = 7.4 Hz, 1H), 7.84 - 7.79 (m, 1H), 7.79 - 7.72 (m, 2H), 7.71-7.65 (m, 3H), 6.72-6.66 (m, 2H), 6.08 (s, 2H). ^{13}C NMR (150 MHz, DMSO-d_6) δ 168.7, 154.1, 153.4, 139.2, 136.9, 134.9, 132.5, 129.4, 129.0, 126.3, 123.2, 121.81, 113.9, 109.4; HRMS calculated for $C_{16}H_{12}N_3O_3S_2$: 358.0315, found 358.0324.

3-((5-(3-Methoxyphenyl)-4H-1,2,4-triazol-3-yl)thio)benzo[b]thiophene 1,1-dioxide (5p)

Prepared from thiol **4o** (50.0 mg, 0.24 mmol) and 2 (68.0 mg, 0.28 mmol) according to general procedure E. Yield 19 mg (19%); light yellow solid; MS (ESI) m/z (%): 372.4 [M+H]$^+$. ^{1}H NMR (600 MHz, DMSO-d_6) δ 7.95 (d, J = 7.5 Hz, 1H), 7.81 (t, J = 7.5 Hz, 1H), 7.74 (q, J = 7.5 Hz, 2H), 7.67 - 7.57 (m, 2H), 7.48 (t, J = 7.8 Hz, 1H), 7.19 (s, 1H), 7.10 (d, J = 8.3 Hz, 1H), 3.85 (s, 3H). ^{13}C NMR (150 MHz, DMSO-d_6) δ 160.0, 137.2, 135.0, 134.6, 132.6, 132.2, 131.0, 130.8, 130.0, 125.1, 122.8, 122.5, 121.4, 119.0, 116.7, 111.7, 55.8; HRMS calculated for $C_{17}H_{13}N_3O_3S_2$: 372.0309, found 372.0309.

3-((5-(3-Methoxyphenyl)-1H-imidazol-2-yl)thio)benzo[b]thiophene 1,1-dioxide (5q)

Prepared from thiol 4p (50.0 mg, 0.24 mmol) and **2** (68.0 mg, 0.28 mmol) according to general procedure E. Yield 19 mg (19%); light yellow solid; MS (ESI) m/z (%): 371.4 [M+H]$^+$. ^{1}H NMR (600 MHz, DMSO-d_6) δ 7.98 - 7.91 (m, 2H), 7.79 (td, J = 7.6, 1.2 Hz, 1H), 7.76 - 7.69 (m, 2H), 7.39 (dd, J = 7.2, 5.2 Hz, 2H), 7.30 (t, J = 7.9 Hz, 1H), 6.82 (d, J = 7.8 Hz, 1H), 6.76 (s, 1H), 3.80 (s, 3H). ^{13}C NMR (150 MHz, DMSO-d_6) δ 160.06, 145.2, 137.4, 134.6, 132.3, 130.18, 129.8, 122.7, 121.7, 121.5, 117.2, 113.0, 110.0, 55.5; HRMS calculated for $C_{18}H_{14}N_2O_3S_2$: 371.0518, found 371.0518.

Synthesis of N-(4-(5-(((1,1-Dioxidobenzo[b]thiophen-3-yl)thio)-1,3,4-oxadiazol-2-yl)phenyl)acetamide (**5o**) To solution of **5n** (25.0 mg, 0.069 mmol) in 3 mL of anhydrous THF, triethylamine (7 mg, 0.070 mmol) was added at room temperature. The reaction mixture was stirred for 5 mins and cooled to 0 °C and acetyl chloride (54 mg, 0.070 mmol) was added dropwise. The reaction mixture was then warmed to room temperature and stirred for 1 h. The

reaction completion was monitored by LC-MS and excess THF was evaporated *in vacuo*. The residue obtained was dissolved in 3 mL of DMSO/Acetonitrile (3:1) and loaded onto a C18 column (GRACE Flash) for purification using water/acetonitrile as a mobile phase. The pure fractions containing product were collected and lyophilized to get **5o**. Yield 6 mg (22%); white solid; MS (ESI) *m/z* (%): 400.2 [M+H]$^+$. ^{1}H NMR (600 MHz, DMSO-d_6) δ 10.37 (s, 1H), 8.02-7.96 (m, 3H), 7.86-7.80 (m, 3H), 7.79-7.75 (m, 2H), 7.72 (s, 1H), 2.10 (s, 3H). ^{13}C NMR (150 MHz, DMSO-d_6) δ 169.4, 167.8, 155.8, 143.5, 139.0, 136.8, 134.9, 132.5, 129.4, 128.4, 126.6, 123.3, 121.8, 119.4, 117.6, 24.6; HRMS calculated for $C_{18}H_{14}N_3O_4S_2$: 400.0420, found 400.0422.

5. Expression and Purification of *C. neoformans* and human IMPDH:

C. neoformans IMPDH was produced by recombinant expression in *E. coli* BL21 (DE3) pLysS and purified as described previously.[27] Human IMPDH isoforms I and II were inserted into pMCSG7 using ligation independent cloning.[28] The enzymes were expressed in *E. coli* BL21 (DE3) pLysS in autoinduction media at 37 °C for approximately 8 h, with shaking at 220 rpm.[29] After expression, cells were harvested and the protein was purified as described previously,[27] except that the His-tag was cleaved using the tobacco etch virus protease (0.4 mg, at 4°C, overnight) and a reverse immobilized metal affinity chromatography step was included to remove His-tagged contaminants before size exclusion chromatography.

6. IMPDH enzymatic assay

Each assay contained 50 mM Tris-HCl, pH 8, 150 mM KCl, 2 mM EDTA, 2% DMSO, 0.0025% Tween-20 and 0.005% BSA, 0.2 μM IMPDH, in addition to 500 μM IMP and NAD for *Cryptococcus* IMPDH and 100 μM NAD and 125 μM IMP for human IMPDH I and II. Reactions were performed in 96-well UV-star flat bottom plates (Greiner Bio-one, Austria) in a POLAR star Omega Plate Reader (BMG LABTECH, Germany) and initiated by addition of

IMP. The rate of NADH was followed at 340 nm ($\varepsilon = 6.22$ mM^{-1}cm^{-1}) production in the presence of each compound at a particular concentration was determined and the enzyme activity calculated by the equation below:

$$NADH\ mM/\min = \frac{Initial\ velocity\ (A_{340}/min)}{Extinction\ coefficient\ NADH\ (6.22\ mM^{-1}cm^{-1})} \times 1\ cm \qquad (1)$$

$$U/mg = \frac{NADH\ mM/min}{Concentration\ of\ IMPDH\ (mg/ml)} \qquad (2)$$

All synthesized compounds and the positive control MPA (all 1 mM stocks in DMSO) were tested 20 to 0.02 μM (for *Cryptococcus* IMPDH) and 30 to 0.93 μM (for hIMPDH I and II). Controls with no inhibitor and 20 μM MPA (resulting in complete inhibition of the enzyme) were used to calculate the percent activity and this was plotted against the log inhibitor concentration and fitted as the log(inhibitor) *vs* normalized response - variable slope equation (3) in Prism version 6 (GraphPad, San Diego, California) to determine the IC$_{50}$. All plates were checked for uniform wells and had a Z'-factor >0.5.[30]

$$y = \frac{100}{(1+10^{(x-\log IC50)})} \qquad (3)$$

Where y is the % activity of the enzyme and x is the log molar concentration of the compound.

7. Enzyme inhibition kinetics:

Kinetics studies of *Cryptococcus* IMPDH with substrates (IMP and NAD) and compound **5d** and **5j** were carried out in the same way as IC$_{50}$ assays, by monitoring the absorbance at 340 nM of NADH produced from the reaction. For K_m determination, reactions were performed using the previously reported assay buffer [50 mM Tris-HCl (pH 8.0), 100 mM KCl, 3 mM EDTA, 1 mM DTT] with concentrations of IMP and NAD varying from 5000 μM to 39 μM and fixed second substrate concentrations of 500 μM for IMP and 700 μM for NAD. All reactions were initiated by the addition of the IMPDH enzyme, reaching a final concentration

32

of 100 nM in the total volume. The rate of reaction and enzyme activity for all reactions were calculated by using the extinction coefficient value of NADH ($\varepsilon = 6.22$ mM^{-1}cm^{-1}). The data was fitted to the Michaelis-Menten equation (Equation 4) by non-linear regression analysis using GraphPad Prism version 7.00 for Windows, GraphPad Software, La Jolla California USA (www.graphpad.com).

$$v = \frac{V_{max}[X]}{K_m + [X]} \qquad (4)$$

Where substrate inhibition was observed ([NAD]>1300 μM), the data was fitted to a modified Michaelis-Menten equation (Equation 5)

$$v = \frac{V_{max}[X]}{K_m + [X]\left(1 + \frac{[X]}{K_i}\right)} \quad (5)$$

where v is the initial velocity; V_{max} is the maximum enzyme velocity; K_m is the Michaelis-Menten constant; $[X]$ is substrate concentration; and K_i is the dissociation constant for substrate binding accounting for two-substrate binding to the enzyme.

Inhibition kinetics analyses were performed in an assay buffer without DTT [50 mM Tris-HCl (pH (8.0), 100 mM KCl, 3 mM EDTA], because compounds **5a**-**5o** showed degradation in the presence of DTT. MPA is an inhibitor of IMPDH from all species and was tested at four different concentrations (312 nM, 156 nM, 78 nM, 39 nM) in reactions with concentration of IMP varying from 25 μM to 800 μM in the presence of 700 μM NAD in one set of reactions, and with NAD varying from 31.25 μM to 1300 μM in the presence of 500 μM IMP in another set of reactions. Compounds **5d** and **5j** were also tested under the same settings as MPA but at eight different concentrations (20 μM, 10 μM, 5 μM, 2.5 μM, 1.25, 0.62 μM and 0.31 μM) to determine the type of inhibition. All inhibition assays were performed in 96-well plates (Greiner Bio-one, Austria) using a Spectramax 190 microplate reader (Molecular devices, Sunnyvale, CA 94089 USA). The enzyme activity data was as described above, and the type

33

of inhibition was evaluated by determining the changes in K_m and V_{max} values in the absence and the presence of the inhibitors.

8. Antifungal assay

Based on a standard MIC assay, all the synthesized test compounds along with standard antifungals (amphotericin B and fluconazole) were serially diluted two-fold across the wells of 96-well NBS plates to determine their antifungal activity. The concentrations of standard antifungals ranged from 256 μg/mL to 0.12 μg/mL and of the test compounds from 512 μg/mL to 0.24 μg/mL, with final volumes of 50μL per well, plated in duplicate. Then, 50 μL of a fungi suspension that was previously prepared in YNB broth to the final concentration of 2.5×10^3 CFU/mL, was added to each well of the compound-containing plates, giving a final standard antifungal concentration range of 128 μg/mL to 0.06 μg/mL, and test compound concentration range from 256 μg/mL to 0.12 μg/mL. Plates were covered and incubated at 35 °C for 24 h. *Candida albicans* MICs were determined by OD530 readings. For *Cryptococcus neoformans,* 10 μL of 0.06% resazurin were added to the 24 h incubated plates, and these plates incubated for another 3 h. *Cryptococcus neoformans* MICs were determined by reading OD570-600. Inhibition of fungal growth was determined by comparison with the negative growth control wells (media only, calculated as an average n = 12) and growth control wells (fungi not treated with antifungals, calculated as an average n = 12). The readings above the negative growth control average were considered to correspond to fungal growth, therefore correspond to active compounds.

9. Cytotoxicity assay

The cytotoxicities of compounds on the HEK293 and HepG2 cell lines were measured by seeding cells with count of 3000 per well in a clear 384-well plate and final volume of 20 mL in the DMEM medium (GIBCO-Invitrogen #11995-073), to which 10% of FBS was added. The compounds were tested with a concentration of 10 mM. A 2-fold dilution series was

prepared and mixed with the cell suspension directly. Then the cells and compounds were incubated for 24 h at 37°C in 5% CO_2. After the incubation, 10 μM resazurin (dissolved in PBS) was added to each well. The plates were then incubated for 3 hours at 37°C in 5% CO_2. The fluorescence intensity was read using Polarstar Omega with excitation/emission 560/590 nm.

10. Mass spectrometry studies

Intact mass spectrometry

For intact mass spectrometry studies, separate samples were prepared for enzyme-only His-tagged *Cryptococcus* IMPDH, His-tagged *Cryptococcus* IMPDH incubated with inhibitor (**5d**: 40 μM in DMSO) and His-tagged *Cryptococcus* IMPDH incubated together with inhibitor **5d** and different combinations of substrates (IMP and NAD independently and with both IMP and NAD). Samples were set up in the same buffer [50 mM Tris-HCl (pH (8.0), 100 mM KCl, 3 mM EDTA] used for inhibition assays and incubated for 1.5 h on ice (4 % final DMSO concentration). A small aliquot (~20 μL) of each sample was prepared for analysis by desalting using a C4 ZipTip (Merck Millipore). Samples were eluted from ZipTip with 10 μL of 80% ACN/0.1% FA, dried briefly in a speed-vac and resuspended in 20 μL buffer A (1 % ACN/0.1% FA). All prepared samples were analysed using an Orbitrap Elite (Thermo) mass spectrometer and Dionex Ultimate 3000 nano LC system (Thermo). Samples were first desalted on a C4 PepMap 300 pre-column (300 μm x 5 mm, 5μm 300 Å) using buffer A (30 μL/min) for 5 min and separated on an Acclaim PepMap 300 (75 μm × 150 mm) at a flow rate of 300 nL/min. A gradient of 10-98% buffer B over 15 minutes was used, where buffer A was 0.1% formic acid in water and buffer B was 80% acetonitrile/0.1% formic acid. The eluted protein was directly analysed on an Orbitrap Elite (Thermo) mass spectrometer interfaced with a NanoFlex source. The mass spectrometer was operated in positive ion mode using the ion trap analyser. Source parameters included an ion spray voltage of 2 kV, temperature at 275°C, SID = 35V, S-lens =

35

70 V, summed microscans = 10, and intact protein mode on. MS analysis was performed across *m/z* 600-2000. Data was deconvoluted using Thermo Protein Deconvolution software™ across mass *m/z* 700-1500. Deconvoluted data was reported as uncharged monoisotopic masses.

Peptide sequencing

Proteomics studies were performed for inhibitor-free His-tagged *Cryptococcus* IMPDH and His-tagged *Cryptococcus* IMPDH incubated with the inhibitor **5d**. The preparation of samples of *Cryptococcus* IMPDH with inhibitor **5d** and incubation for 1.5 h on ice and incubation at room temperature was done in similar manner to samples prepared for intact mass spectrometry studies. After incubation, the solution was transferred to Amicon Ultra centrifugal filter (10 KDa, Millipore) and centrifuged at 4 ℃ to remove any excess unbound inhibitor in the sample. The protein was transferred to an Eppendorf tube and trypsin (Promega, V5111) added at a concentration of 1:25 (w/w), along with ammonium bicarbonate to a final concentration of 50 mM. The sample was incubated at 37 ℃ overnight. The protein-only sample was also digested with trypsin in parallel. After incubation, a small aliquot (~5 µg) of each sample was taken and prepared for analysis by desalting using a C18 ZipTip.

Digested samples were separated using reverse-phase chromatography on a Dionex Ultimate 3000 RSLC nano-system. Using a flow rate of 30 µL/min, samples were desalted on a Thermo PepMap 100 C18 trap (0.3 × 5 mm, 5 µm) for 5 min, followed by separation on a Acclaim PepMap RSLC C18 (150 mm × 75 µm) column at a flow rate of 300 nL/min. A gradient of 10-50% buffer B over 27 min was used to separate peptides (buffer A corresponded to 1 % acetonitrile / 0.1% formic acid and buffer B corresponded to 80% ACN / 0.1% FA). Eluted peptides were directly analysed on an Orbitrap Elite mass spectrometer (Thermo) using an NSI electrospray interface. Source parameters included a capillary temperature of 275 °C; S-Lens RF level at 60%; source voltage of 2 kV and maximum injection times of 200 ms for MS and 150 ms for MS2. Instrument parameters included an FTMS scan across *m/z* range 350-1800 at

36

60,000 resolution, followed by information-dependent acquisition of the top 10 peptides across *m/z* 40-1800. Dynamic ion exclusion was employed using a 15-second interval. Charge state screening was enabled with rejection of +1 charged ions and monoisotopic precursor selection was enabled.

Data was converted to Mascot generic format (mgf) using the msConvert software (ProteoWizard) and searched using Protein Pilot™ v5.0 (Sciex).[31,32] A custom database containing His-tagged IMPDH was generated. The unique modification expected for cysteine residues ($C_8H_5O_2S$, +164 Da) was added to the database.

ASSOCIATED CONTENT

Supporting Information.

Supplemental information includes synthesis of methyl 4-(hydrazinecarbonyl)benzoate (**3f**), mass spectra of IMPDH peptide fragments from enzyme-only and compound **5d**-treated sample.

Author Contributions

A.A.B.R., and M.A.C. guided to design the synthetic chemistry and L.K.K. conducted them. J.A.F., B.K., E.F. and R.B. designed experiments for overexpression and purification of *Cryptococcus* and human IMPDHs and E.F., R.B. performed them. U.K. and E.F. guided to perform enzyme assays and L.K.K. conducted them. A.N., M.S.B. and B.K. helped to plan mass spectrometry experiments and A.N. performed the experiments. A.N. and L.K.K. analyzed the mass spectrometry data. L.K.K wrote the paper and all authors reviewed and revised the manuscript.

ACKNOWLEDGMENT

ABBREVIATIONS

IMPDH, Inosine monophosphate dehydrogenase; HTS, High-throughput screening; Dithiothreitol, DTT; PAINS, pan-assay interference compounds; IMP, Inosine-5′-monophosphate; XMP, Xanthosine-5′-monophosphate; NAD, Nicotinamide adenine dinucleotide; MPA, mycophenolic acid.

REFERENCES

1. Atherton G. Fungal Infection Trust https://www.fungalinfectiontrust.org/ (accessed March **2018**).

2. Ianiri G and A. Idnurm. Essential gene discovery in the basidiomycete *Cryptococcus neoformans* for antifungal drug target prioritization. mBio. **2015**, 6(2): e02334-02314.

3. Vázquez-González, D, et al. Opportunistic yeast infections: candidiasis, cryptococcosis, trichosporonosis and geotrichosis. *J. Dtsch. Dermatol. Ges*. **2013**, 11(5): 381-394.

4. Centers for Disease Control and Prevention. *Cryptococcus*: Screening for Opportunistic Infection among People Living with HIV/ AIDS. Retrieved from https://www.cdc.gov/fungal/pdf/at-a-glance-508c.pdf (accessed March **2018**)

5. Lin X and J. Heitman. The biology of the *Cryptococcus neoformans* species complex. *Annu. Rev. Microbiol.* **2006**, 60(1): 69-105.

6. Liu T.-B. et al. Molecular mechanisms of cryptococcal meningitis. *Virulence*. **2012**, 3(2): 173-181.

7. Roden M. M. et al. Triad of acute infusion-related reactions associated with liposomal amphotericin B: analysis of clinical and epidemiological characteristics. *Clin. Infect. Dis*. **2003**, 36(10): 1213-1220.

8. Hamill R. J, Amphotericin B formulations: A comparative review of efficacy and toxicity. *Drugs*. **2013**, 73(9): 919-934.

9. Larsen R. A et al. Amphotericin B and Fluconazole, a potent combination therapy for Cryptococcal meningitis. *Antimicrob. Agents Chemother*. **2004**, 48(3): 985-991.

10. Perfect J. R, The antifungal pipeline: a reality check. *Nat. Rev. Drug Discov*. 2017, 16: 603.

11. Hedstrom L. IMP Dehydrogenase: Structure, mechanism, and inhibition. *Chem. Rev*., **2009**, 109(7): 2903-2928.

12. Morrow C. A, et al. *De novo* GTP biosynthesis is critical for virulence of the fungal pathogen Cryptococcus neoformans. *PLoS Pathogens*. **2012**, 8(10): e1002957.

13. Dahlin J. L. et al. PAINS in the assay: chemical mechanisms of assay interference and promiscuous enzymatic inhibition observed during a sulfhydryl-scavenging HTS. *J. Med. Chem*. **2015**, 58(5): 2091-2113.
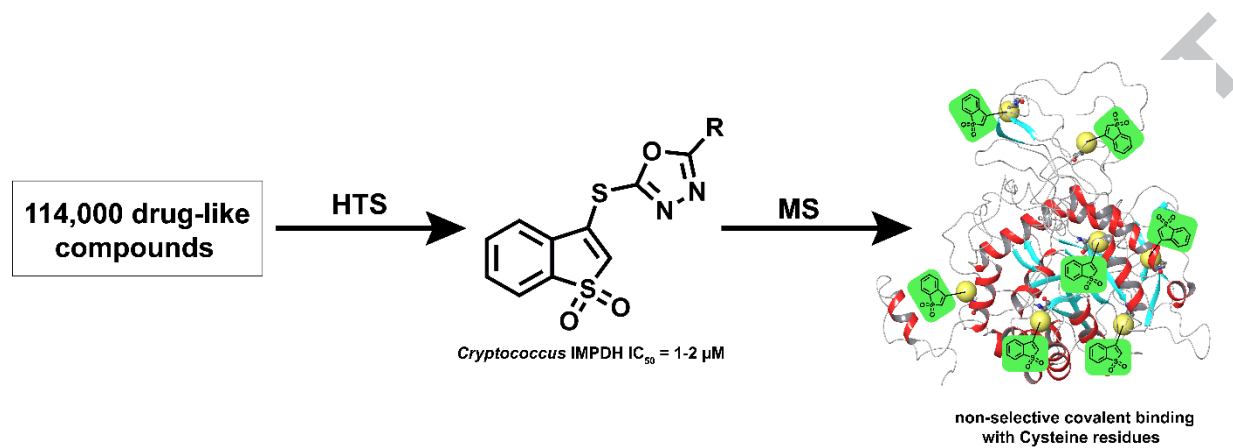
14. Dahlin JL, Baell J, Walters MA. Assay interference by chemical reactivity. In: Sittampalam GS.; Coussens NP.; Brimacombe K, et al.; editors. Assay Guidance Manual [Internet]. Bethesda (MD): Eli Lilly & Company and the National Center for Advancing Translational Sciences. **2015** Sep 18. Available from: https://www.ncbi.nlm.nih.gov/books/NBK326709/

15. Dahlin J. L. et al. Assay interference and off-target liabilities of reported histone acetyltransferase inhibitors. *Nat. Commun.* **2017**, 8(1): 1527. doi:10.1038/s41467-017-01657-3

16. Pouliot M, and S. Jeanmart. Pan Assay Interference Compounds (PAINS) and other promiscuous compounds in antifungal research. *J. Med. Chem*. **2016**, 59(2): 497-503.

17. Verma A. K. et al. A general and efficient CuI/BtH catalyzed coupling of aryl halides with thiols. *Tetrahedron Lett*. **2007**, 48(40): 7199-7202.

18. Soleiman-Beigi M. et al. A Combined synthetic and DFT study on the catalyst-free and solvent-assisted synthesis of 1,3,4-oxadiazole-2-thiol derivatives. *Journal of Chemistry*. **2013**, 6.

19. Yar M. S. et al. Synthesis and anti tuberculostatic activity of novel 1,3,4-oxadiazole derivatives. *J. Chinese Chem. Soc*. **2007**, 54(1): 5-8.

20. Li P. et al. Antibacterial activities against rice bacterial leaf blight and tomato bacterial wilt of 2-mercapto-5-substituted-1,3,4-oxadiazole/thiadiazole derivatives. *Bioorganic Med. Chem. Lett*. **2015**, 25(3): 481-484.

21. Chen L. et al. Triazole-linked inhibitors of Inosine Monophosphate Dehydrogenase from human and Mycobacterium tuberculosis. *J. Med. Chem.* **2010**, 53(12): 4768-4778.

22. Makowska-Grzyska M. et al. Bacillus anthracis Inosine 5′-Monophosphate Dehydrogenase in action: The first bacterial series of structures of phosphate ion-, substrate-, and product-bound complexes. *Biochem.* **2012**, 51(31): 6148-6163.

23. Riera T. V et al. Allosteric activation via kinetic control: Potassium accelerates a conformational change in IMP Dehydrogenase. *Biochem.* **2011**, 50(39): 8508-8518.

24. Zhou X et al. Expression, Purification, and Characterization of Inosine 5′-Monophosphate Dehydrogenase from Borrelia burgdorferi. *J. Biol. Chem.* **1997**, 272(35): 21977-21981.

25. Wilkins M.R, Lindskog I, Gasteiger E, Bairoch A, Sanchez J.-C, Hochstrasser D.F, and Appel R.D. Detailed peptide characterisation using PEPTIDEMASS - a World-Wide Web accessible tool. *Electrophoresis.* **1997**, 18(3-4), 403-408.

26. Gasteiger E, Hoogland C. Gattiker A, Duvaud S, Wilkins M.R, Appel R.D, Bairoch A. Protein Identification and Analysis Tools on the ExPASy Server. (In) John M. Walker (ed): The Proteomics Protocols Handbook, Humana Press. **2005**, pp. 571-607.

27. Morrow C. A. et al. Crystallization and preliminary X-ray analysis of mycophenolic acid-resistant and mycophenolic acid-sensitive forms of IMP dehydrogenase from the human fungal pathogen Cryptococcus. *Acta Crystallographica* Section F. **2010**, 66(9): 1104-1107.

28. Stols L, Gu M, Dieckman L, Raffen R, Collart, F. R and Donnelly M. I. A new vector for high-throughput, ligation-independent cloning encoding a tobacco etch virus protease cleavage site. *Protein Expr. Purif.* **2002**, 25, 8-15.

29. Studier F. W. Protein production by auto-induction in high-density shaking cultures. *Protein Exp. Purif.* **2005**, 41, 207–234.

30. Zhang JH, Chung TD, Oldenburg KR, A Simple Statistical Parameter for Use in Evaluation and Validation of High Throughput Screening Assays. *J. Biomol. Screen*. **1999**, 4(2), 67-73.

31. Shilov IV, Seymour SL. et al. The Paragon Algorithm, a next generation search engine that uses sequence temperature values and feature probabilities to identify peptides from tandem mass spectra. *Mol. Cell. Proteomics*. **2007**, 6(9):1638-55.

32. Tang WH, Shilov IV, Seymour SL. Nonlinear fitting method for determining local false discovery rates from decoy database searches. *J. Proteome Res*. **2008**, 7(9):3661-7.

<u>Graphical abstract</u>

non-selective covalent binding
with Cysteine residues